

# Platinum Nanoparticles on Sintered Metal Fibers Are Efficient Structured Catalysts in Partial Methane Oxidation into Synthesis Gas

Andrei Tarasov, Natalia Root, Olga Lebedeva, Dmitry Kultin, Liubov Kiwi-Minsker, and Leonid Kustov\*



Cite This: *ACS Omega* 2020, 5, 5078–5084



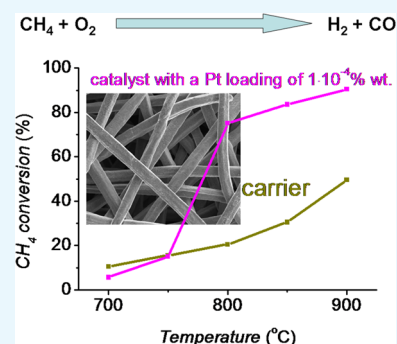
Read Online

ACCESS |

Metrics & More

Article Recommendations

**ABSTRACT:** Efficient structured catalysts of partial methane oxidation into synthesis gas were obtained by electrochemical modification of the surface of sintered FeCrAl alloy fibers in an ionic liquid BMIM-NTf<sub>2</sub> with further introduction of platinum nanoparticles. It was shown that etching and electrochemical modification of sintered FeCrAl alloy fibers result in a decrease of the surface aluminum content. With an increase of the reaction temperature to 900 °C, the methane conversion reaches 90% and the selectivity to CO increases significantly to achieve 98%. The catalysts with a Pt loading of  $1 \times 10^{-4}$  wt % demonstrate high activity and selectivity as well as TOF in synthesis gas production by the CH<sub>4</sub> + O<sub>2</sub> reaction at 850–900 °C. To trace the composition and structure evolution of the catalysts, XRD and SEM methods were used.



## 1. INTRODUCTION

The reaction of partial oxidation of methane into synthesis gas (POM) rendering the molar ratio H<sub>2</sub>/CO = 2 in the products is considered as a valuable alternative to methane steam reforming and one of the reactions in the so-called “trireforming” process.<sup>1,2</sup> The mechanism of POM depends on the nature of the catalytic active phase, its dispersion, and oxidation state, thus influencing the selectivity of the catalytic process.<sup>3</sup> Moreover, the reaction is highly exothermic, and a perfect control of the thermal regime is required for the process efficiency.

The heat exchange between the catalyst and the reaction gas mixture can be significantly improved by applying a catalytic carrier with a high thermal conductivity, such as structured metal supports: metallic gauzes, foils, foams, and fibers. They present also developed surface area and high thermal and mechanical stability combined with an open structure allowing a low pressure drop through the catalytic bed.<sup>4</sup> Among such carriers, the recently studied Fe-Cr-Al (FeCrAl alloy) sintered metal fibers (SMF) of porous sheets<sup>5–8</sup> formed by uniform micro-sized filaments present high porosities up to 80–90%. Since the original FeCrAl alloy SMFs do not have sufficient surface area (the SSA may reach 1–2 m<sup>2</sup>/g only), the application of this material as a carrier requires surface modification that may be achieved by special treatment, for instance, by high-temperature oxidation or acid treatment.<sup>2–9</sup> The enhancement of the specific surface area of the metallic carrier is beneficial for supporting active metals at high dispersion.

Surface treatment of metals by IL under the electrochemical control is known to result in the formation of surface nanostructures (cells, nanotubes, etc.).<sup>10,11</sup> Unlike the high-temperature treatment, this method of modification can be used at room temperature, and the surface organization can be controlled by using different parameters, such as the current, potential, addition of chemical agents, and time of treatment.

Another important issue for efficiency of POM process is the catalyst resistance toward coke formation.<sup>12</sup> Coking leads not only to catalyst deactivation but increases the pressure drop through the catalytic bed diminishing the POM process efficiency. In this concern, the metallic structured catalysts are robust alternative to bulk catalysts.<sup>1,2</sup> The use of the open structure of sintered metal fibers with their surface being coated with a porous oxide layer serving as a carrier for metal nanoparticles should result in a suppression of the catalyst deactivation due to coke formation.

It was shown<sup>13</sup> that the product yields in the POM reaction on a Pt/CeO<sub>2</sub>-ZrO<sub>2</sub> catalyst prepared by impregnation with an aqueous solution of PtCl<sub>4</sub> is virtually independent of the platinum loading. Electrochemical methods of metal deposition, including noble metals, like platinum, exhibit a number of advantages, in addition to the energy economy, compared to

Received: November 26, 2019

Accepted: February 21, 2020

Published: March 6, 2020



other methods of preparation of supported metal catalysts. First, by varying the current or potential, one can prepare deposits with a controlled dispersion on the electrode surface. Second, ultralow loaded metal deposits (lower than 0.05–0.1 wt %) can be obtained. Finally, the amount of deposited metal can be easily controlled and calculated on the basis of the Faraday law.

The goal of this research is the development of an efficient structured catalyst based on FeCrAl-alloy SMF. The catalyst was prepared by electrochemical modification of SMF in an ionic liquid followed by electrochemical deposition of platinum. The obtained catalysts were characterized by different physicochemical methods, and their catalytic properties were tested in the methane oxidation to synthesis gas.

## 2. RESULTS AND DISCUSSION

The electrochemical modification of the surface of sintered metal fibers in an ionic liquid has been studied in detail.<sup>14</sup> It has been found that anodic modification affects the formation of surface nanostructures in different ways. In the case of SMF1, the increase of the current and time of anodization results in electrochemical etching, whereas in the case of SMF2, the surface polishing takes place. The process of etching of the original FeCrAl sample in an acid may influence the depth of the natural surface oxide layer, thereby affecting the specific surface area of the carrier and adhesion of the deposits.<sup>15</sup>

The use of the slope of the transient (the  $E-t$  dependence) in the starting time interval (up to 10 ms)<sup>16,17</sup> allows one to estimate the thickness of the surface oxide layer on the metal by the formula

$$\delta = \frac{\varepsilon \varepsilon_0}{C} \quad (1)$$

where  $\delta$  is the thickness of the layer,  $\varepsilon$  is the dielectric constant,  $\varepsilon_0$  is the dielectric constant of vacuum, and  $C$  is the capacity. The capacity was determined from the transient as the ratio  $q/\Delta E$  for the starting linear segment of the  $E-t$  dependence.

Three oxide layers have been observed on the surface of FeCrAl by transmission electron microscopy:<sup>17</sup> the outer layer of  $\text{Al}_2\text{O}_3$ , the middle layer of  $\text{Al}_{1.98}\text{Cr}_{0.02}\text{O}_3$ , and the deep layer of  $\text{AlFeO}_3$ . The surface oxide on FeCrAl represents not a simple oxide but a mixture of several phases; therefore, determination of the  $\varepsilon$  value is a problem. Thus, it seems reasonable to determine not the  $\delta$  value but the variation of the thickness upon different treatments.

It is possible to estimate the variation of the thickness of the oxide layer arising as a result of modification of the surface of SMF1 by anodization in ionic liquid using the dependences presented in Figure 1 (inset). The ratio of the thickness of the original oxide layer to the thickness after the modification ( $\delta_0/\delta_1$ ) is 1.3. The thickness of the surface oxide layer is decreased by ~25%. Compared to the sample SMF1, the thickness of the surface oxide layer after the treatment in HCl (sample SMF2) is reduced by 25%. On the contrary, for the sample SMF2, the anodization in the ionic liquid results in an increase in the thickness of the surface oxide layer by 50%.

Table 1 summarizes the data on the surface composition of the original sample (SMF1), the sample SMF1 treated in HCl (sample SMF2), and the sample SMF2 modified by anodization in the ionic liquid (IL).<sup>14</sup>

The chemical etching and electrochemical modification of sintered FeCrAl fibers in the ionic liquid result in a decrease in

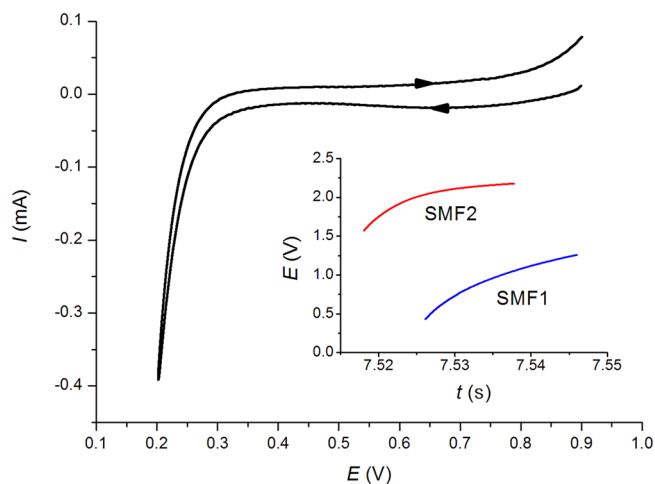


**Figure 1.** Electrochemical behavior of SMF samples: voltammograms ( $I-E$  dependences) for sample SMF1 in a 1% aqueous solution of  $\text{H}_2\text{PtCl}_6$  acidified with HCl to pH = 1, sweep rate 1 mV/s. Inset: transients ( $E-t$  dependences) at a constant current of  $I = 8$  mA for the unmodified sample SMF1 and for the modified ( $I = 8$  mA,  $t = 300$  s) sample SMF2 in BMIM-NTf<sub>2</sub>.

the surface content of aluminum and, as a result, an increase in the relative content of molybdenum (Table 1). The XPS study of the original and modified (with platinum) materials revealed two states of iron in all the samples under study:  $\text{Fe}^0$  and  $\text{Fe}_2\text{O}_3$  and/or  $\text{Fe}_3\text{O}_4$ , whereas chromium is present in the state  $\text{Cr}_2\text{O}_3$  and/or  $\text{CrO}_2$ . Thus, it has been established that the surface of SMF is covered with iron and chromium oxides.  $\text{Fe}_2\text{O}_3$  and  $\text{Cr}_2\text{O}_3$  are known to be poorly soluble in hydrochloric acid. Hydrogen released upon the dissolution of  $\text{Fe}^0$  may cause reduction and dissolution of iron oxide. This results in a decrease in the depth of the surface oxide layer after etching with hydrochloric acid. In the case of ionic liquids, the anodic behavior of metals is different from that in aqueous solutions.<sup>14</sup>

In order to investigate the process of electrodeposition of platinum on FeCrAl from a 1 wt % aqueous solution of  $\text{H}_2\text{PtCl}_6$  acidified with HCl, cyclic voltammograms of the samples were measured (Figure 1). The low sweep rate for the potential of the working electrode provides a quasi-stationary profile of the current and the potential. The value of the initial potential ( $E = 0.9$  V) excludes the possibility of spontaneous deposition of platinum. The slow variation of the potential in the range of 0.9–0.35 V corresponds to the limiting stage of the mass transfer.<sup>18</sup> The fast decrease of the current at potentials below 0.35 V corresponds to the platinum deposition. The cathodic and anodic branches of the voltammograms demonstrate a hysteresis. The anodic branch is higher than the cathodic branch, which is typically related to the electrochemical formation and growth of a new phase after nucleation.

The original samples SMF1, SMF2, and the samples obtained from SMF1 and SMF2 after modification with BMIM-NTf<sub>2</sub> were applied further as carriers for electrochemical deposition of Pt. The catalytic tests of samples SMF1 and SMF2 after Pt deposition were depicted elsewhere.<sup>14</sup> The images of the surfaces of the original carriers SMF1 and SMF2 and the corresponding Pt catalysts produced using these carriers (after modification with BMIM-NTf<sub>2</sub>) at different

Table 1. Chemical Composition of the Sintered FeCrAl Fiber Samples under Study Determined by XPS

element composition, wt %	Al	Si	Cr	Mn	Fe	Ni	Mo
original SMF1	0.71	0.45	17.92	0.12	68.38	9.66	2.87
SMF1 treated in HCl (SMF2)	0.14	0.30	18.14	0.25	68.66	9.78	2.98
SMF2 electrochemically treated in the IL	0.08	0.36	18.00	0.26	67.61	9.77	3.90

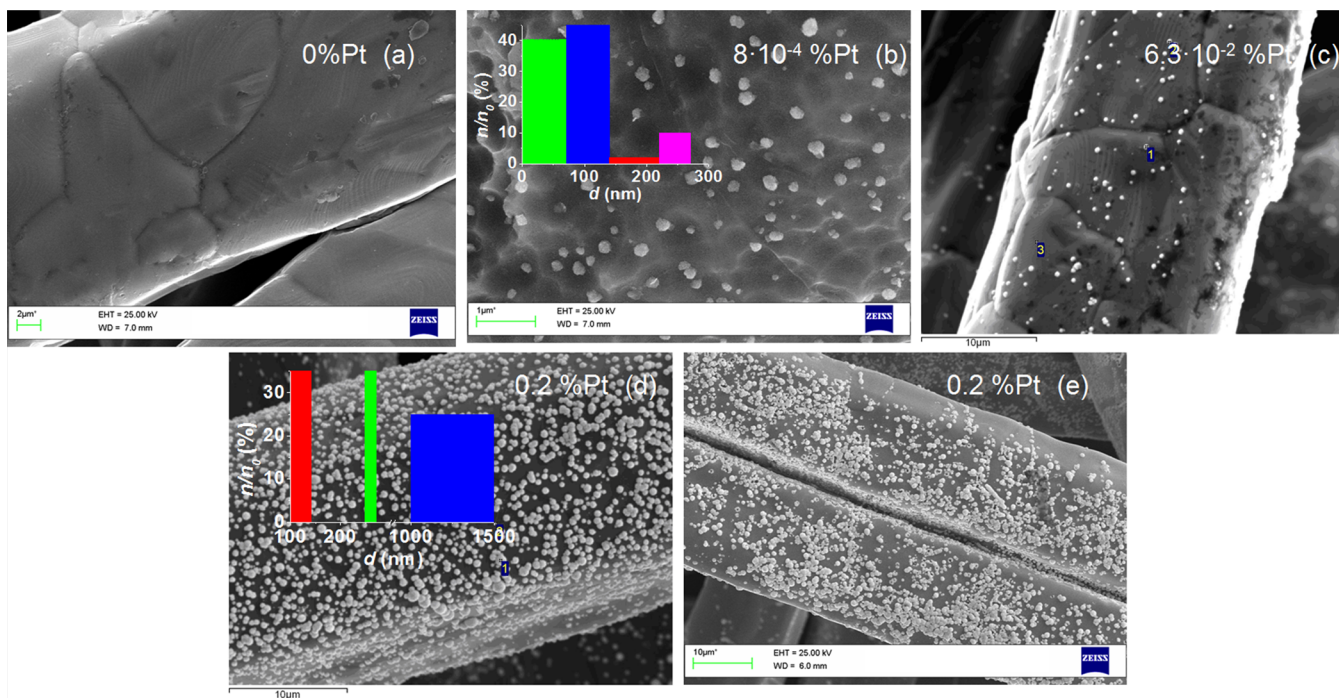


**Figure 2.** SEM images of the original FeCrAl sample (SMF1) (a) and the samples obtained from SMF1 after modification with BMIM-NTf<sub>2</sub> and further electrochemical deposition of platinum at different currents and time intervals: (b)  $i = -2.7 \text{ mA/cm}^2$ ,  $t = 300 \text{ s}$ ; (c)  $i = -4 \text{ mA/cm}^2$ ,  $t = 300 \text{ s}$ ; (d)  $i = -40 \text{ mA/cm}^2$ ,  $t = 20 \text{ s}$ ; (e)  $i = -80 \text{ mA/cm}^2$ ,  $t = 10 \text{ s}$ . Insets for panels (b) and (e): Pt particle size distributions.

currents and time intervals of platinum deposition are shown in Figures 2 and 3.

It is seen that the coverage of the surface by platinum increases with the increase of the current density. The lower the current density, the lower is the concentration of two-dimensional nuclei formed at the surface. At a very low current density, it is possible to assume the formation only of the two-dimensional nucleus that further grows to cover the entire surface of the cathode (Figure 3b,c). When the current density increases and the concentration of ad-ions grows, the number of two-dimensional nuclei increases too. The high current density provides a sufficient overpotential at the electrode and, as a result, a larger number of nuclei<sup>14</sup> (Figure 2e,f,d).

The size of Pt particles on initial catalysts was determined by electron microscopy. Figure 3b (inset) demonstrates the Pt particle size distribution for the catalyst containing  $1 \times 10^{-4}$  wt % Pt (b).

An increase of the current leads to the formation of larger agglomerates with a size of 1000–1500 nm (25% of the total number of Pt particles) (Figure 2d,e). However, the share of the particles with a smaller size is significant: 35% of 250–270 nm and 35% of 100–140 nm (Figure 2d). The distribution was determined using 225 Pt particles. For the sample SMF2 (Figure 3), a similar pattern is observed, that is, agglomeration of Pt particles on the catalyst with the formation of large Pt agglomerates of microsize.

The platinum dispersion ( $D$ ) can be calculated by the formula

$$D = \frac{6C_a M_{\text{Pt}} 10^9}{\rho d_p N} \quad (2)$$

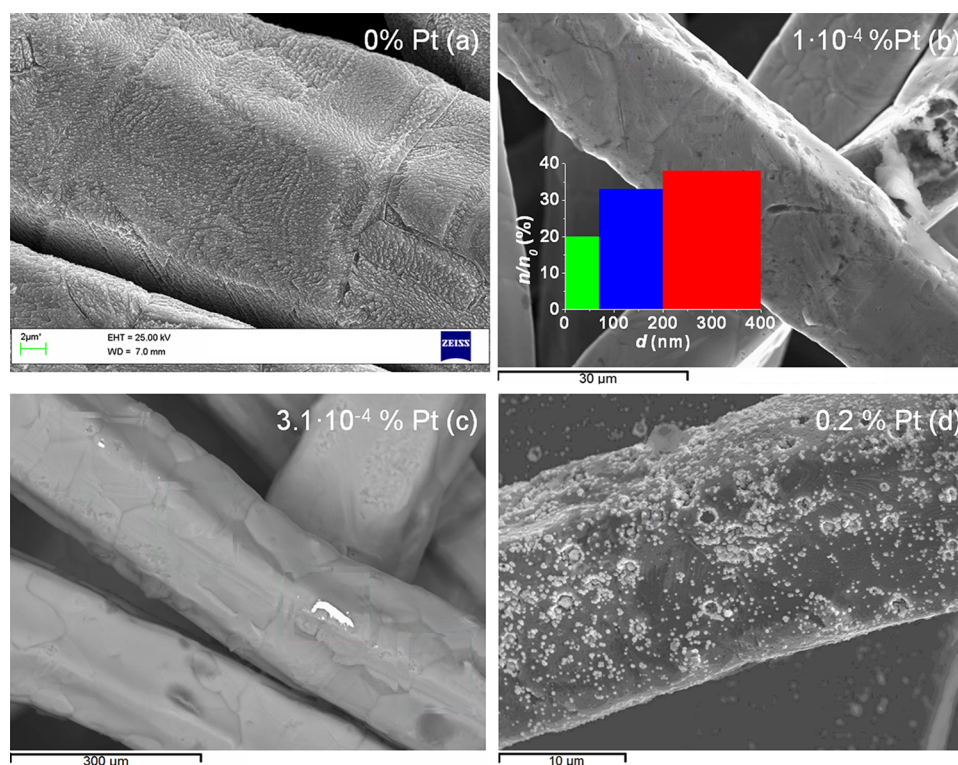
where  $C_a$  is the surface concentration of metal equal to  $1.31 \times 10^{19}$  atoms per  $1 \text{ m}^2$ ,  $M_{\text{Pt}}$  is the mass of the Pt atom ( $\text{g mol}^{-1}$ ),  $\rho$  is the volume density of platinum,  $21.09 \times 10^6 \text{ g M}^{-3}$ ,  $N$  is Avogadro's number,  $D$  is the metal dispersion, and  $d_p$  is the diameter of nanoparticles approximated as semispheres.<sup>19</sup> For Pt nanoparticles with a mean diameter of 70 nm, the dispersion is 1.7%. For the catalyst  $1 \times 10^{-4}$  wt % Pt/SMF2, platinum particles represent agglomerates with a size of about 10 nm, which corresponds to a dispersion of about 13%. According to the XPS data, platinum is present in the Pt<sup>0</sup> state.

Figure 4 demonstrates the characteristics of the partial methane oxidation reaction for the carrier (SMF2) and the composite catalyst  $1 \times 10^{-4}$  wt % Pt/SMF2.

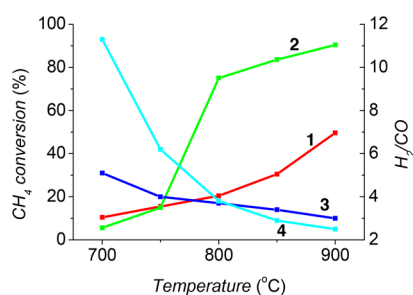
It is seen from Figure 4 that the FeCrAl carrier exhibits some catalytic activity. The activity of the composite catalyst increases drastically above 800 °C, and the reaction proceeds with the formation of the optimal H<sub>2</sub>/CO mixture close to the molar ratio of 2.

Table 2 summarizes the results of the catalytic tests in the reaction of partial methane oxidation into synthesis gas on the catalysts with a different platinum loading on the carriers SMF1 and SMF2.

It follows from the data of Table 2 that the original and modified FeCrAl carriers (SMF1 and SMF2) exhibit some activity in the POM reaction. The methane conversion on the



**Figure 3.** SEM images of the starting sample SMF2 (a) and the samples obtained from SMF2 after modification with BMIM-NTF<sub>2</sub> and further and after electrochemical deposition of platinum at different currents and time intervals: (b)  $i = -0.05 \text{ mA/cm}^2$ ,  $t = 20 \text{ s}$  (inset: Pt particle size distribution); (c)  $i = -5 \text{ mA/cm}^2$ ,  $t = 20 \text{ s}$ ; (d)  $i = -80 \text{ mA/cm}^2$ ,  $t = 10 \text{ s}$ .



**Figure 4.** Dependence of the methane conversion (%) and the H<sub>2</sub>/CO molar ratio for the carrier SMF2 (1, 3, respectively) and the composite catalyst 1 × 10<sup>-4</sup>% Pt/SMF2 (2, 4, respectively) vs temperature. Reaction conditions: VHSV of the mixture at the molar ratio O<sub>2</sub>/CH<sub>4</sub> = 0.48 was 8000 h<sup>-1</sup>.

unmodified metal carriers reached 30–50% with the selectivity toward CO about 70–80%. The conversion can be increased to 90–95% at a higher temperature (1000–1100 °C); however, the metallic carriers start to destroy under such severe conditions. Etching of the SMF surface results in an increase of the methane conversion and selectivity to CO. Presumably, this is caused by an increase of the specific surface area of the carrier (SMF2) after the HCl treatment as compared to the unmodified sample SMF1 (Figures 2a and 3a). Deposition of platinum results in an increase of the catalytic activity. The samples containing 1 × 10<sup>-4</sup> and 3.1 × 10<sup>-4</sup>% Pt on SMF2 demonstrate exceptionally high specific activity (per gram of platinum) as compared to the samples with higher Pt loadings (Table 2). For these catalysts, the molar ratio H<sub>2</sub>/CO is close to 2, being suitable for methanol synthesis (Figure 4). The higher catalytic activity of these catalysts is likely due to a

**Table 2.** Pt Contents and Catalytic Activities of the Composite Catalysts Based on FeCrAl Sintered Fibers in Partial Methane Oxidation into Synthesis Gas<sup>a</sup>

catalyst	H <sub>2</sub> /CO ratio	CH <sub>4</sub> conversion (vol %)	selectivity to CO <sup>b</sup> (%)	TOF <sup>c</sup> (s <sup>-1</sup> )
original carrier SMF1 ( $S = 15 \text{ cm}^2$ )	3.4	30.5	71.7	
8 × 10 <sup>-4</sup> % Pt/SMF1	2.5	41.6	81.7	86.9
6.3 × 10 <sup>-2</sup> % Pt/SMF1	3.2	60.8	62.7	1.61
0.2% Pt/SMF1	3.4	57.6	61.4	0.48
modified carrier SMF2	3.4	49.6	81.5	
1 × 10 <sup>-4</sup> % Pt/SMF2	2.2	90.4	98.1	1510.7
3.1 × 10 <sup>-4</sup> % Pt/SMF2	2.0	56.0	63.7	301.9
1.1 × 10 <sup>-3</sup> % Pt/SMF2	3.3	58.4	61.4	83.7

<sup>a</sup>Reaction conditions:  $T = 900 \text{ °C}$ , VHSV of the mixture at the molar ratio O<sub>2</sub>/CH<sub>4</sub> = 0.48 was 8000 h<sup>-1</sup>. <sup>b</sup>The other carbon-containing product was CO<sub>2</sub>, its selectivity being equal to (100 - S<sub>CO</sub>)%. <sup>c</sup>Calculated as the number of CH<sub>4</sub> molecules converted per 1 atom of loaded platinum per second.

**Table 3. Contents of Elements for the  $8 \times 10^{-4}\%$  Pt/SMF1 and  $1.1 \times 10^{-3}\%$  Pt/SMF2 Catalysts after the Catalytic Tests<sup>a</sup>**

catalyst	C	O	Cr	Mn	Fe	Ni
$8 \times 10^{-4}\%$ Pt/SMF1 (wt %)	$1.50 \times 10^{-3}$	$1.16 \times 10^{-2}$	6.89	0.12	71.99	7.00
$1.1 \times 10^{-3}\%$ Pt/SMF2 (wt %)	$1.54 \times 10^{-3}$	$4.74 \times 10^{-3}$	5.92	0.24	77.78	8.33

<sup>a</sup>The content of Pt after the catalytic tests decreases insignificantly and is about  $7 \times 10^{-4}$  wt % for both samples.

higher Pt metal dispersion. In the case of the  $1 \times 10^{-4}\%$  Pt/SMF2 catalyst (inset in Figure 3b), platinum particles represent agglomerates of smaller nanoparticles, which corresponds to a dispersion of about 13% (compared with a dispersion of 1.7% for 0.2% Pt/SMF1). It was shown<sup>19</sup> for palladium composite catalysts with metal dispersion ranging from 11 to 30% that the maximum specific catalytic activity in the reaction of methane conversion is observed at a dispersion of 18%.

The corrosion behavior of FeCrAl alloys at high temperatures in O<sub>2</sub> or O<sub>2</sub> + H<sub>2</sub>O media has been studied recently in detail.<sup>20,21</sup> It has been shown that the surface of the FeCrAl alloy is covered by an aluminum oxide (corundum) layer formed at high temperatures protecting the alloy from progressive corrosion.<sup>20,21</sup> According to the data of Tables 1 and 3, the surface aluminum content in the samples under study is very low (below 1%). Iron and chromium oxides are present at the surface. Figure 5a,b presents SEM images of the

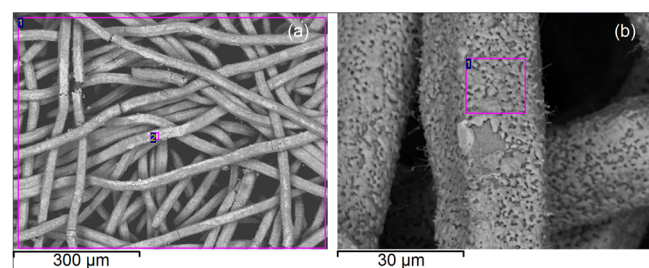


**Figure 5.** SEM images of the spent  $8 \times 10^{-4}\%$  Pt/SMF1 catalysts at different magnification: (a) general view and (b) enlarged fragment.

areas of the alloy surface after catalysis. Table 3 summarizes the data on the surface contents of certain elements in the cell with sizes of  $10 \mu\text{m} \times 10 \mu\text{m} \times 1 \mu\text{m}$  for the spent catalyst shown in Figure 5.

It follows from Table 3 that the catalytic reaction is accompanied by a negligible soot formation if compared to the conventional granulated Pt catalysts on porous supports. Indeed, the carbon content is about 1.5 wt % only. Typically, the coke content in the catalyst under conditions of partial methane oxidation or reforming (steam or dry reforming) may reach 15–30 wt %.<sup>22</sup> A possible reason behind the low coke formation in the case of the structured catalysts is the process of fouling of coke precursors due to the open structure of the catalysts.<sup>23</sup>

### 3. CONCLUSIONS

1. The electrochemical modification of the surface of sintered FeCrAl alloy fibers in an ionic liquid was studied for the first time. It was found that the depth of the surface oxide layer after the anodization in the ionic liquid decreases for the sample that was not preliminarily treated with hydrochloric acid. For the pretreated fibers under the same conditions, the depth of the surface oxide layer increases. Etching and electrochemical

modification of sintered FeCrAl alloy fibers result in a decrease of the surface aluminum content.

2. At low temperatures (700 °C), methane is mainly oxidized on the FeCrAl catalysts with or without platinum to produce CO<sub>2</sub>. With an increase of the reaction temperature to 900 °C, the methane conversion increases by about 4 times with a significant increase of the selectivity to CO up to 98%.
3. The catalysts with a Pt loading of  $1 \times 10^{-4}$  wt % Pt demonstrated complete methane conversion, with the synthesis gas composition of H<sub>2</sub>/CO = 2 being suitable for the downstream methanol synthesis. The TOF value for this catalyst exceeds the TOFs for other samples by 1–3 orders of magnitude.
4. The structured Pt catalysts based on sintered FeCrAl alloy fibers demonstrate a very low coke formation contrary to the supported granulated Pt catalysts.

### 4. MATERIALS AND METHODS

**4.1. Preparation of Catalysts.** Sintered FeCrAl metal fibers (SMFs) with a composition of Fe(73)Cr(20)Al(5) pressed (shaped) in the form of sheets (30 × 60 mm, thickness 0.29 mm, Southwest Screens & Filters SA, Belgium), a fiber diameter of 0.02 mm, open porosity of 0.7, specific surface area (Ar) of 2 m<sup>2</sup>/g were used for the preparation of catalysts.

The original sintered metal fibers (SMF1) and the samples treated for 15 min with concentrated HCl for comparison (SMF2) were used for supporting platinum by electrochemical deposition.

Electrochemical studies were carried out using an Autolab PGSTAT302N potentiostat. Electrochemical anodization was performed in a three-electrode electrochemical cell in air at room temperature. Ionic liquid (1-butyl-3-methylimidazolium bis(triflate)imide, BMIM-NTEF<sub>2</sub>, purity 99%, the water content 220 ppm) was supplied by ABCR GmbH. SMF sheets, either pretreated in HCl or untreated samples with the surface of  $S = 15 \text{ cm}^2$ , served as the working electrode (anode). A stainless-steel plate ( $S = 15 \text{ cm}^2$ ) was used as an auxiliary electrode. Silver wire was applied as a reference electrode. Electrochemical oxidation was carried out at a constant current of  $I = 60 \text{ mA}$  for 60, 300, 600, or 900 s. Then the electrodes were washed with bidistillate water and acetone and dried until constant weight. The procedure for the electrochemical modification of the surface of samples SMF1 and SMF2 in ionic liquids under conditions of the anodization with variation of the time and current of the treatment resulting in the formation of a diversity of nanostructures at the surface was described elsewhere.<sup>14</sup> In the studies with ionic liquid, platinum and silver wire were used as an auxiliary electrode and a quasi-reversible reference electrode, respectively. The potential of the silver wire was constantly calibrated versus a standard  $\text{fc}/\text{fc}^+$  electrode.

The catalysts were prepared by electrodeposition of platinum from a 1% aqueous solution of H<sub>2</sub>PtCl<sub>6</sub> acidified with HCl onto the surface of the modified samples SMF1 and

SMF2. Deposition of platinum was carried out at the cathode current density  $i = -2.7$  to  $-80$  mA/cm<sup>2</sup> for 10–300 s using a two-electrode scheme.

The choice of the conditions of deposition was based on the Faraday law. The average weight of the SMF sheet was 0.6 g. In order to support 0.001% or 1 wt % Pt, the quantity of electricity of about 0.012 or 12 C, respectively, is required. This value was achieved by varying the current and deposition time, for example,  $i = -0.05$  mA/cm<sup>2</sup>,  $t = 20$  s. This current density corresponds to  $I = -0.7$  mA,  $Q = 1.4$  C, and  $m(\text{Pt}) = 7 \times 10^{-7}$  g or  $1 \times 10^{-4}\%$  Pt. This catalyst was labeled as  $1 \times 10^{-4}\%$  Pt/SMF2.

Scanning electron microscopy (SEM) measurements were carried out using an LEO EVO-50 XVP Zeiss Techniques EDX analyzer. The element analysis of the surface was carried out using energy-dispersive microanalysis with an INCA Energy 350 (Oxford Instruments) detector at 15 kV.

**4.2. Procedure of Catalytic Measurements.** The catalysts were tested in the reaction of particle methane oxidation into synthesis gas at an atmospheric pressure in a plug-flow quartz reactor (i.d. 5 mm) in the temperature range of 700–1000 °C. The volume hourly space velocity at the molar ratio  $\text{O}_2/\text{CH}_4 = 0.48$  was 8000 h<sup>-1</sup> (as calculated per volume of the cylindrical catalytic block, that is, SMF sheet scrolled to form a cylindrical block with a volume of 1 cm<sup>3</sup> (height 15 mm, diameter 5 mm).

Analysis of the gas mixture at the reactor outlet was determined by gas chromatography using a 3700 (NPO Granat) chromatograph in isothermal mode (70 °C) using a thermal conductivity detector and two packed columns: with molecular sieve 5A (H<sub>2</sub>, O<sub>2</sub>, N<sub>2</sub>, CH<sub>4</sub>, and CO) and HayeSep-Q (CO<sub>2</sub>). Helium served as a carrier gas. The analysis was performed according to the procedure described elsewhere.<sup>1,2</sup>

## AUTHOR INFORMATION

### Corresponding Author

Leonid Kustov – Zelinsky Institute of Organic Chemistry, 119991 Moscow, Russia; Department of Chemistry, Lomonosov Moscow State University, 119991 Moscow, Russia; Science and Technology University “MISIS”, 119049 Moscow, Russia; [orcid.org/0000-0003-2312-3583](https://orcid.org/0000-0003-2312-3583); Email: [lmkustov@mail.ru](mailto:lmkustov@mail.ru)

### Authors

Andrei Tarasov – Zelinsky Institute of Organic Chemistry, 119991 Moscow, Russia

Natalia Root – Department of Chemistry, Lomonosov Moscow State University, 119991 Moscow, Russia

Olga Lebedeva – Department of Chemistry, Lomonosov Moscow State University, 119991 Moscow, Russia; [orcid.org/0000-0003-2333-660X](https://orcid.org/0000-0003-2333-660X)

Dmitry Kultin – Department of Chemistry, Lomonosov Moscow State University, 119991 Moscow, Russia

Liubov Kiwi-Minsker – Ecole Polytechnique Federale, 1015 Lausanne, Switzerland; Tver Technical State University, 170026 Tver, Russia; [orcid.org/0000-0002-7192-7212](https://orcid.org/0000-0002-7192-7212)

Complete contact information is available at:

<https://pubs.acs.org/10.1021/acsoomega.9b04020>

### Notes

The authors declare no competing financial interest.

## ACKNOWLEDGMENTS

This work was supported by the Ministry of Education and Science of the Russian Federation in the framework of Increase Competitiveness Program of NUST MISIS (grant no. K2-2019-005) in the part related to catalytic studies and Russian Science Foundation (project 17-13-01526) in the part related to the preparation of catalysts.

## ABBREVIATIONS

IL, ionic liquid; SEM, scanning electron microscopy; SMF1, original sintered metal fibers; SMF2, the samples of sintered metal fibers treated with concentrated HCl.

## REFERENCES

- (1) Tarasov, A. L.; Kustov, L. M. Partial methane oxidation into synthesis gas over catalysts supported on meshed metallic materials. *Catal. Chem. Petrochem Ind.* **2013**, *5*, 14–20.
- (2) Tarasov, A. L.; Kustov, L. M.; Lishchiner, I. I.; Malova, O. V.; Eremeeva, O. S.; Kivi, L. L. Method for preparing a catalyst for gas synthesis from methane, a catalyst prepared by this method, and a method of producing gas synthesis from methane with its use. RU. Patent 2,619,104(C1), May 12, 2017.
- (3) Usachev, N. Y.; Kharlamov, V. V.; Belanova, E. P.; Starostina, T. S.; Krukovskii, I. M. Oxidative processing of light alkanes: State-of-the-art and prospects. *Russ. J. Gen. Chem.* **2009**, *79*, 1252–1263.
- (4) Danilova, M. M.; Kuzin, N. A.; Kirillov, V. A.; Sobjanin, V. A.; Sabirova, Z. A.; Brizitskij, O. F.; Terent'ev, V. J.; Khristoljubov, A. P.; Khrobostov, L. N. Catalyst, method for preparation thereof, and a synthesis gas generation method. RU. Patent 2,268,087(C1), January 20, 2006.
- (5) Turco, R.; Haber, J.; Yuranov, I.; Russo, V.; Santacesaria, E.; Kiwi-Minsker, L. Sintered metal fibers coated with transition metal oxides as structured catalysts for hydrogen peroxide decomposition. *Chem. Eng. Process.* **2013**, *73*, 16–22.
- (6) Makarshin, L. L.; Gribovskij, A. G.; Andreev, D. V.; Parmon, V. N. Catalytic micro-passage plates and method of their making. RU. Patent 2,323,047(C1), April 27, 2008.
- (7) Wang, Y.; Tonkovich, A. L. Y.; Vanderwiel, D. P. Catalyst and method of steam reforming. U.S. Patent 6,958,310(B2), October 25, 2005.
- (8) Tonkovich, A. L. Y.; Wang, Y.; Gao, Y. Catalyst, method of making, and reactions using the catalyst. U.S. Patent 6,762,149(B2), July 13, 2004.
- (9) Sigaeva, S. S.; Tsyryl'nikov, P. G.; Shlyapin, D. A.; Dorofeeva, T. S.; Voitenko, N. N.; Vershinin, V. I.; Davletkil'deev, N. A.; Kuznetsov, G. B.; Kanashenko, S. L. Catalysts of methane pyrolysis: Pretreatment and study of FeChal support. *Russ. J. Appl. Chem.* **2009**, *82*, 307–311.
- (10) Lebedeva, O.; Kultin, D.; Kudryavtsev, I.; Root, N.; Kustov, L. The role of initial hexagonal self-ordering in anodic nanotube growth in ionic liquid. *Electrochem. Commun.* **2017**, *75*, 78–81.
- (11) Abbott, A. P.; Capper, G.; McKenzie, K. J.; Ryder, K. S. Voltammetric and impedance studies of the electropolishing of type 316 stainless steel in a choline chloride based ionic liquid. *Electrochim. Acta* **2006**, *51*, 4420–4425.
- (12) Tsodikov, M. V.; Kurdjumov, S. S.; Bukhtenko, O. V.; Zhdanova, T. N. Method of producing catalyst of methane-bearing hydrocarbon steam conversion. RU. Patent 2,483,799(C2), June 10, 2013.
- (13) Pantu, P.; Kim, K.; Gavalas, G. R. Methane partial oxidation on Pt/CeO<sub>2</sub>-ZrO<sub>2</sub> in the absence of gaseous oxygen. *Appl. Catal. A: Gen* **2000**, *193*, 203–214.
- (14) Kustov, L. M.; Lebedeva, O. K.; Kultin, D. Y.; Root, N. V.; Kazansky, V. B. Electrochemical modification of steel by platinum nanoparticles. *Dokl. Chem.* **2016**, *470*, 297–301.
- (15) Bakanov, V. I.; Larina, N. V. Electrochemical forming nanostructures: thin films of bismuth. *Izv. Vyssh. Uchebn. Zaved., Khim. Khim. Tekhnol.* **2012**, *55*, 59–62 (in Russian).

- (16) Lohrengel, M. M. Thin anodic oxide layers on aluminium and other valve metals: high field regime. *Mater. Sci. Eng., R: Rep* **1993**, *11*, 243–294.
- (17) Kim, D. H.; Yu, B. Y.; Cha, P. R.; Yoon, W. Y.; Byun, J. Y.; Kim, S. H. A study on FeCrAl foam as effective catalyst support under thermal and mechanical stresses. *Surf. Coat. Technol.* **2012**, *209*, 169–176.
- (18) Chen, S.; Kucernak, A. Electrodeposition of platinum on nanometer-sized carbon electrodes. *J. Phys. Chem. B* **2003**, *107*, 8392–8402.
- (19) Chen, Z.; Wang, S.; Ding, Y.; Zhang, L.; Lv, L.; Wang, M.; Wang, S. Pd catalysts supported on Co<sub>3</sub>O<sub>4</sub> with the specified morphologies in CO and CH<sub>4</sub> oxidation. *Appl. Catal., A Gen.* **2017**, *532*, 95–104.
- (20) Israelsson, N. Analysis of Condensable Hydrocarbons in Gasification Processes. Ph.D. Thesis, Chalmers University of Technology, Sweden, 2014.
- (21) Park, D. J.; Kim, H. G.; Park, J. Y.; Jung, Y. I.; Park, J. H.; Koo, Y. H. A study of the oxidation of FeCrAl alloy in pressurized water and high-temperature steam environment. *Corros. Sci.* **2015**, *94*, 459–465.
- (22) Freni, S.; Calogero, G.; Cavallaro, S. Hydrogen production from methane through catalytic partial oxidation reactions. *J. Power Sources* **2000**, *87*, 28–38.
- (23) Claridge, J. B.; Green, M. L. H.; Tsang, S. C.; York, A. P. E.; Ashcroft, A. T.; Battle, P. D. A study of carbon deposition on catalysts during the partial oxidation of methane to synthesis gas. *Catal. Lett.* **1993**, *22*, 299–305.